ACS Sustainable Chemistry & Engineering

Research Article

pubs.acs.org/journal/ascecg

# Green Synthesis of Noble Nanometals (Au, Pt, Pd) Using Glycerol under Microwave Irradiation Conditions

Jiahui Kou,*[,†] Christina Bennett-Stamper,[‡] and Rajender S. Varma*[,†]

[†]Sustainable Technology Division, National Risk Management Research Laboratory, U.S. Environmental Protection Agency, 26 West Martin Luther King Drive, MS 443, Cincinnati, Ohio 45268, United States

[‡]Water Supply Water Resources Division, National Risk Management Research Laboratory, U.S. Environmental Protection Agency, 26 West Martin Luther King Drive, MS 681, Cincinnati, Ohio 45268, United States

Supporting Information

**ABSTRACT:** A newer application of glycerol in the field of nanomaterials synthesis has been developed from both the economic and environmental points of view. Glycerol can act as a reducing agent for the fabrication of noble nanometals, such as Au, Pt, and Pd, under microwave irradiation. Their shapes can be changed by adding different surfactants. In the presence of CTAB, Au nanosheets were formed within 2 min where the size of Au nanosheets can be controlled by the microwave irradiation time and glycerol content.

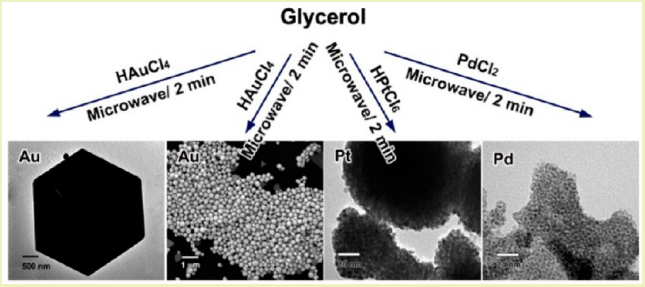


**KEYWORDS:** *Glycerol, Green synthesis, Noble metal, Microwave, Polyol processes*

## INTRODUCTION

As the main coproduct (approximately 10 wt %) of biodiesel production from transesterification of vegetable oils, the generation of glycerol is dramatically increasing with the rapid development of the biodiesel industry.[1,2] It was estimated that approximately 4 billion gallons of crude glycerol would be produced by 2016.[3] The increasing supply of the environmental benign glycerol has cause great interest in its new applications, because of the advantageous from both the economic and environmental points of view. The classical use of glycerol has been within the pharmaceutical, food, and cosmetic industries.[4] Comparatively, however, the investigation of glycerol in the field of nanomaterial synthesis has been largely ignored.

Noble metal nanoparticles with interesting size dependent electrical, optical, magnetic, and chemical properties have been intensively investigated, not only for their fundamental scientific interest, but also for their many technological applications.[5−11] The polyol processes, which exploit high-boiling polyalcohol solvents as reducing agents, are widely used in the synthesis of noble metal nanomaterials with various morphologies because of their simplicity and compatibility in open-air environments.[12−16] Ethylene glycol is the most often used polyalcohol for the polyol process because of its good reactivity for the fabrication of a wide variety of metal nanomaterials.[6,13,17] However, the metabolites of ethylene glycol, glycolic acid, and oxalic acid may cause acute renal failure, cerebral damage, and injury to other organs, which prohibits the widespread use of the polyol process.[18,19] There are three hydrophilic hydroxyl groups in a glycerol molecule. Although the polyol method has been well-investigated, the use of glycerol has been neglected. Recently, we reported the use of glycerol in the polyol process for the speedy fabrication of Ag nanowires. By this means, Ag nanowires could be obtained within 1 min, moreover, the diameter of Ag nanowire can be controlled.[20] Nevertheless, the synthesis of other noble nanometals using the polyol process still needs further investigation.

In the current study, a green methodology using glycerol has been developed for the fabrication of Au, Pt, and Pd nanomaterials under microwave (MW) irradiation. Different surfactants, such as cetyltriethylammnonium bromide (CTAB), polyvinylpyrrolidone (PVP), and sodium dodecyl sulfate (SDS), are used to synthesize samples with different morphologies. In addition, temperature and pressure in the MW system are monitored to investigate their role on the formation of metal nanoparticles.

## EXPERIMENTAL SECTION

**Synthesis of Material.** In a typical procedure, 0.02 g noble metal source ($HAuCl_4$, $HPtCl_6$, or $PdCl_2$), surfactant, and 4 mL water were first mixed in a 10 mL thick walled glass tube reactor, and then, 4 mL glycerol was added dropwise. After that, the thick walled glass tube reactor was sealed with a cap and, then, was irradiated in a CEM Discover focused MW synthesis system maintaining a temperature of 100 °C (monitored by a built-in infrared sensor) for 2 min with a maximum pressure of 280 psi. The resulting precipitated noble metal samples were then washed several times with water and ethanol to remove organics. Similar experiments were carried out by varying the content of reactant, temperature, and reaction time. Control experiments

Special Issue: Sustainable Nanotechnology

Received: January 17, 2013
Revised: February 27, 2013
Published: March 6, 2013

  

under conventional heating condition were conducted in a stainless steel autoclave with Teflon liner and heated in oven at 100 °C for 10 min, the same temperature reached in the MW system.

**Characterization.** The crystal structures of prepared samples were detected by an X-ray diffractometer (Xpert, Pro, Holland). The morphology was examined by transmission electron microscopy (TEM) (JEOL, JEM-2100, Japan), scanned electron microscopy (SEM) (JEOL, JSM-6490LV, Japan), and field emission scanned electron microscopy (FESEM) (JEOL, JSM-7600F, Japan).

**Evaluation of Catalytic Activity of As-Prepared Au Nanosheets.** Catalytic reduction experiments of 4-nitrophenol were performed to evaluate the catalytic efficiency and reusability of prepared Au nanosheets. In a typical experiment, a mixture of 19.5 mL water, 0.5 mL of 10 mM 4-nitrophenol, and 1.25 mmol $NaBH_4$ was first prepared in a 40 mL vial at room temperature, and then 0.01 mmol Au nanosheets was added with magnetic stirring. After completion of the reaction, the reaction mixture was filtered by a Millipore syringe driven filter to get clear solution for UV/vis spectroscopy (Agilent Hewlett-Packard, 8453, USA) analysis. For comparison, the experiment without Au nanosheet was also carried out under similar conditions.

## RESULTS AND DISCUSSION

The XRD pattern of as-prepared Au particles is shown in Figure 1. The peaks at $2\theta$ = 38.3, 44.6, 64.7, and 77.5 for Au nanoparticles are easily indexed, respectively, to the diffraction of the (111), (200), (220), and (311) Au planes (PDF no. 01-1174). SEM was used to detect the morphology of as-prepared Au nanoparticles without stirring, as Figure 2 shows. In the absence of surfactant, particles with the diameter of 500 nm were formed. When the use of CTAB was 0.05 mmol, the hexagonal nanosheets were obtained as well as nanoparticles, and the percentage composition of hexagonal nanosheets was about 50%. With the enhancing of CTAB content, the ratio of nanosheets was increasing, which reached more than 90% in the presence of 0.1 mmol CTAB. However, as the Figure 2d and e displays, excessive CTAB could hinder the formation of Au nanosheets; therefore, the percentage composition of hexagonal nanosheets reduced to about 40% with 0.2 mmol of CTAB. Moreover, it is hard to find Au nanosheets when 0.4 mmol of CTAB was used. If 2 mL ethanol was used to replace 2 mL water, the formation of Au nanosheets also can be destroyed. CTAB is an amphiphilic chemical, which can form a bilayer to permit aqueous solubility. Polar head groups attach CTAB to the Au surface and the bilayers structure also allows polar CTAB head groups to interface with the surrounding water phase and provide aqueous dispersibility.[21] CTAB can influence the Au nanoparticles' growth kinetics along specific crystallographic planes due to its affinity for the Au facet.[22] Usually, CTAB is used in the synthesis of Au nanorods.[23−25] With our method, the Au samples were formed very quickly; therefore, nanosheets were obtained rather than nanorods.

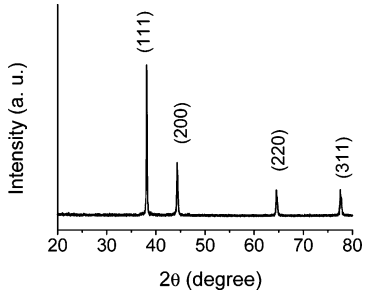


**Figure 1.** XRD pattern of as-prepared Au nanoparticles using glycerol.

It is worth noting that no Au sample can be formed when magnetic stirring was used, which is similar with the result obtained in the Ag preparation system.[20] As Supporting Information Figure S1 shows, when stirring was used, the maximum pressure was just 30 psi, which is much lower than that in the absence of stirring. However, the temperature can reach to 100 °C within 1 min, which is much faster than that in the absence of stirring. As a result, the fact that no Au sample can be formed with stirring should be associated with pressure rather than temperature, same as the Ag system.[20] Under closed

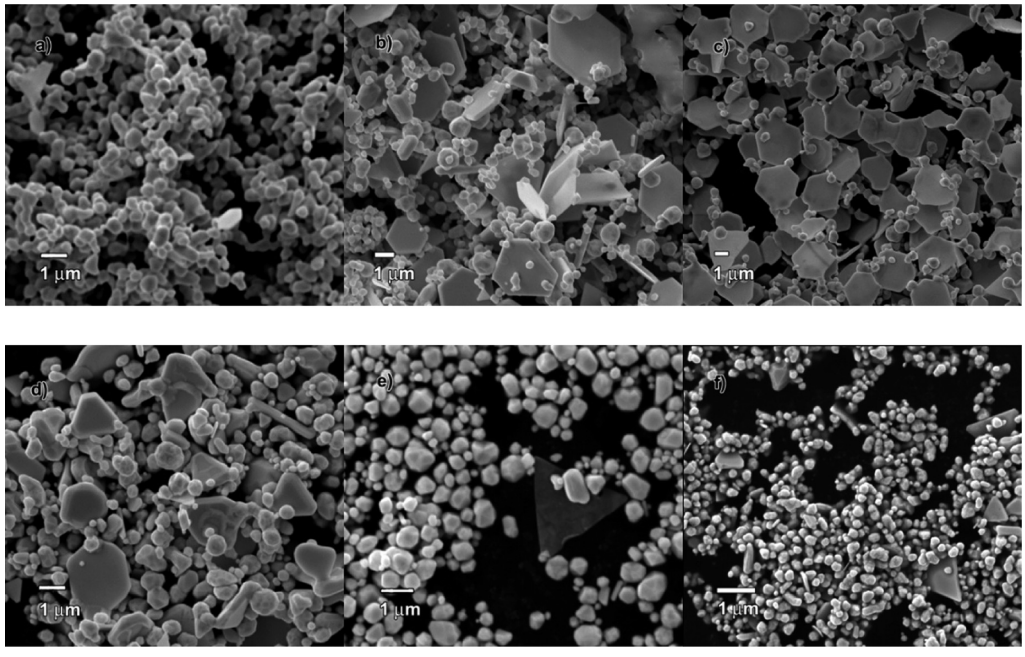


**Figure 2.** SEM images of the as-prepared Au samples with or without surfactant (other chemical: 2 mL Au aqueous solution (10 g/L), 4 mL glycerol, and 2 mL water). (a) no surfactant; (b) 0.05 mmol CTAB; (c) 0.1 mmol CTAB; (d) 0.2 mmol CTAB; (e) 0.4 mmol CTAB; (f) 2 mL ethanol was used to replace 2 mL water, 0.1 mmol CTAB.

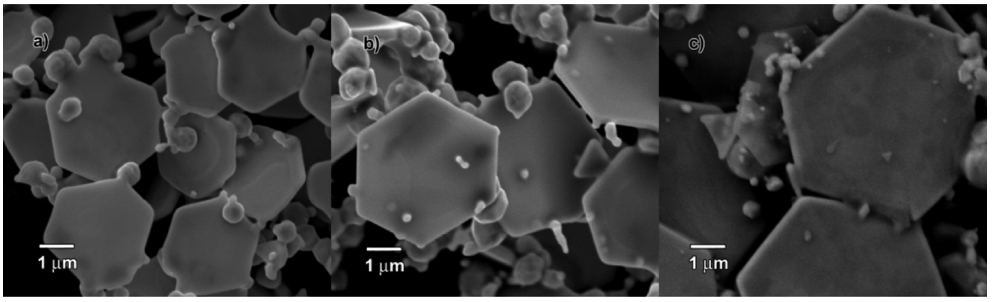


**Figure 3.** SEM images of Au samples obtained at different times: (a) 2; (b) 30; (c) 60 min.

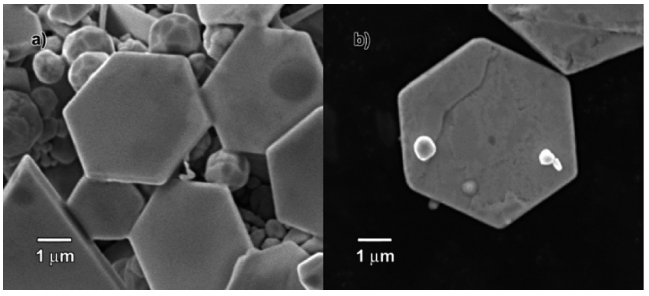


**Figure 4.** SEM images of Au samples obtained using different glycerol content: (a) 2; (b) 1 mL.

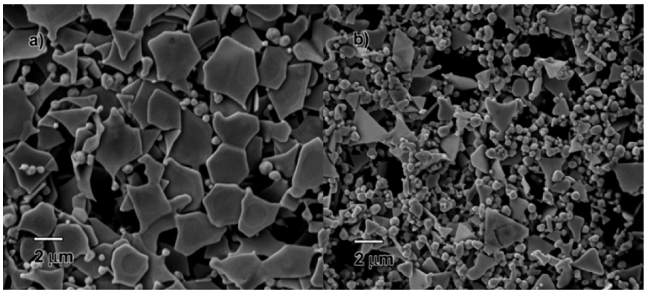


**Figure 5.** SEM images of Au samples obtained using different $HAuCl_4$ (10 g/L) amount: (a) 1; (b) 0.5 mL.

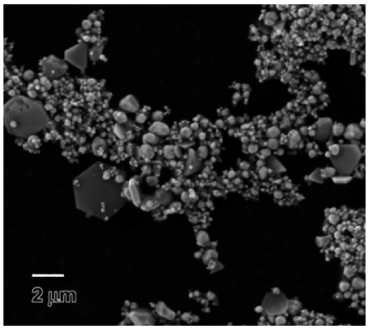


**Figure 6.** SEM images of Au samples obtained at 80 °C.

vessel conditions, reaction mixtures can be heated and maintained at an elevated temperature far above the boiling point of the solvent for several minutes under MW irradiation.[26−29] Consequently, it is much easier to access instant high pressure and generate "hot spots" because of explosive boiling than the traditional heating method.[26−28] However, when the stirring was used, the explosive boiling can be restrained. It is well-known that high pressure and hot spots are helpful to the formation of inorganic materials;[28,30−32] therefore, they should be the most important reasons that Au samples only can be obtained in the system without stirring. Comparatively, experiments under conventional heating conditions were conducted. However, no Au sample was formed after heating at 100 °C for 10 min. These results prove that high pressure and hot spots attained in MW close reaction systems are necessary requisites for the formation of an Au sample.

Reaction time is usually an important influencing factor for morphology control.[30,33] Accordingly, samples prepared at different times were investigated. Figure 3 shows the SEM image of samples formed at different times; the magnification of these samples is the same, 9500×. When the reaction time was 2 min, the side length of hexagonal nanosheets was about 1−1.5 $\mu$m, which could be enhanced with the prolonging of reaction time. As the time was 30 min, the side length was about 2 $\mu$m, while it could reach to 3 $\mu$m at 60 min. The possible reason is that after the formation of Au crystal nucleus, the crystals continue to grow on the surface of existing Au nanosheets. These results indicate that the size of Au hexagonal nanosheets can be controlled by changing the reaction time with this method. The effect of glycerol was also studied. Without glycerol, the Au phase cannot be formed under the same conditions. This fact illustrates the important reducing role of glycerol for the formation of Au in the current conditions. The content of glycerol also plays a significant role in the side length of hexagonal nanosheets (Figure 4). More glycerol can contribute to more formation of crystal nucleus, as a result of which the sizes of Au nanosheets are smaller. As mentioned above, when the use of glycerol was 4 mL (Figure 3a), the side length of hexagonal nanosheets was about 1−1.5 $\mu$m. When 2 mL glycerol was used, the side length was about 2 $\mu$m. Hexagonal nanosheets with side length of 3 $\mu$m were obtained with 1 mL of glycerol. The usage of $HAuCl_4$ was changed to figure out the effect of $HAuCl_4$ content. As illustrated in Figure 2c, when the use of $HAuCl_4$ solution was 2 mL, the shapes of most of the obtained Au nanosheets are hexagonal. However, the shapes of formed Au nanosheets (Figure 5) with 1 mL $HAuCl_4$ are not regular though their thickness is similar with that of 2 mL. When the use of $HAuCl_4$ was 0.5 mL, the shapes of most of the obtained Au samples are triangular nanosheets, whose percentage composition is much lower than that of the 2 and 1 mL. The reaction profile in the MW system with different amounts of $HAuCl_4$ was monitored (Supporting Information Figure S2), indicating that the content of $HAuCl_4$ can affect the temperature and pressure. When the use of $HAuCl_4$ was low (0.5 mL), the temperature cannot reach 100 °C even within 12 min and the pressure of the system was just about 100 psi. With the increasing amount of $HAuCl_4$, the temperature can reach 100 °C sooner. As the use of $HAuCl_4$ was 2 mL, temperature reached 100 °C in 7 min.

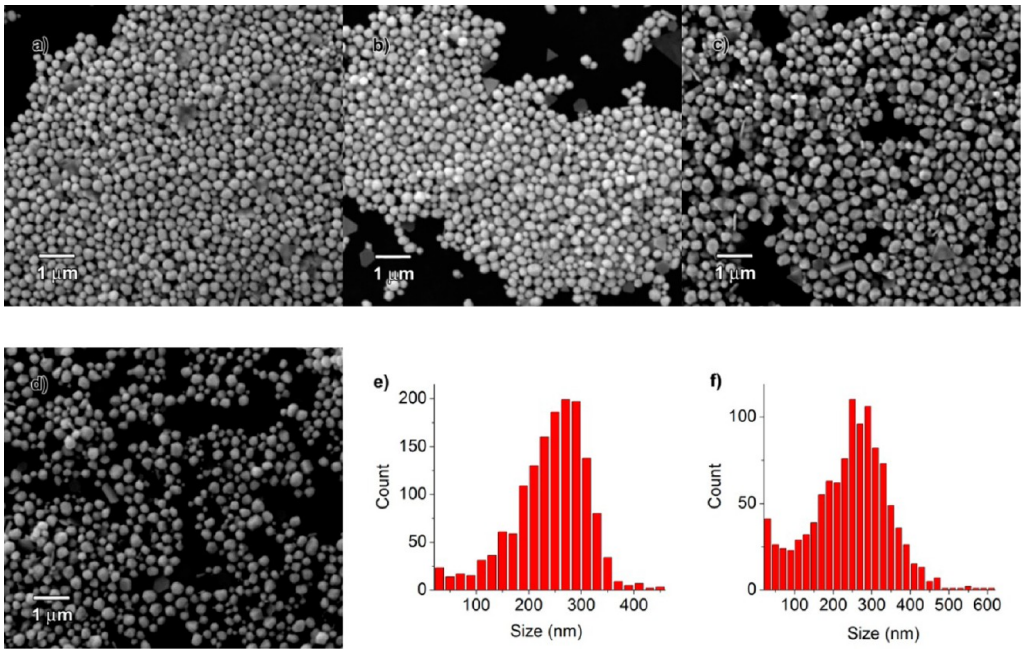


**Figure 7.** (a–d) SEM images of Au samples obtained using different PVP amounts: (a) 0.16; (b) 0.08; (c) 0.04; (d) 0.02 g. (e and f) Size distribution of Au nanoparticles obtained using different PVP amounts: (e) 0.16; (f) 0.02 g.

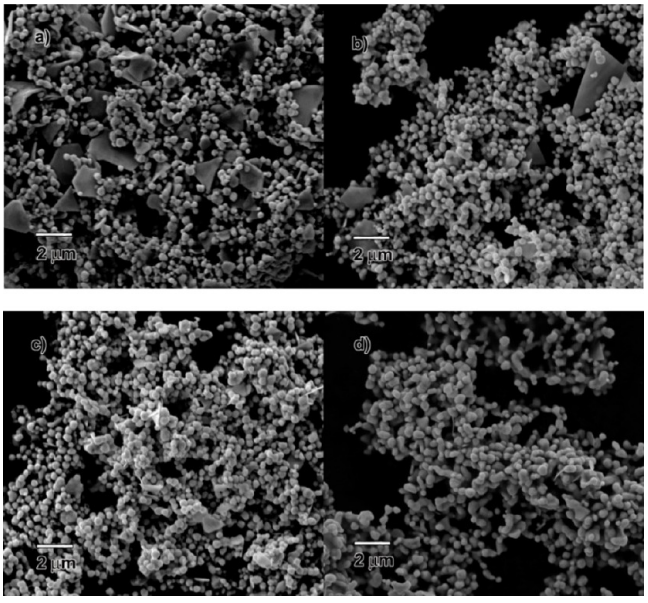


**Figure 8.** SEM images of Au samples obtained using different SDS amounts: (a) 0.6; (b) 0.3; (c) 0.15; (d) 0.075 mmol.

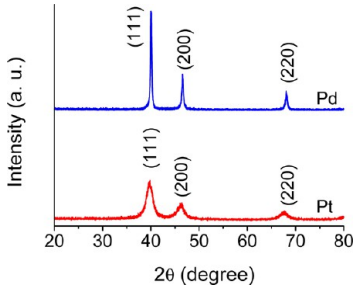


**Figure 9.** XRD patterns of as-prepared Pd and Pt nanoparticles using glycerol under MW irradiation.

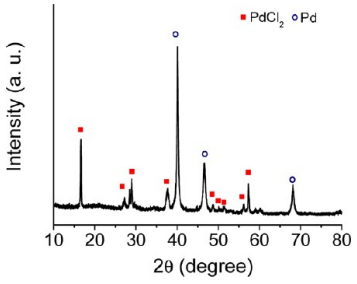


**Figure 10.** XRD pattern of powder obtained in Pd system under conventional heating.

The maximum pressure increased with an increasing amount of $HAuCl_4$, which is about 100 psi with 0.5 mL $HAuCl_4$ and about 250 psi with 2 mL $HAuCl_4$. Therefore, $HAuCl_4$ could absorb MW to contribute to the high temperature and pressure in the system. As mentioned above, pressure plays a crucial role on the formation of metal samples, which may be the reason for the uniform morphology obtained with 2 mL of $HAuCl_4$.

Usually, temperature is significant for material synthesis. Therefore, the effect of different temperatures was investigated. At 100 °C, uniform hexagonal nanosheets were obtained; however, the mixture of nanoparticles and hexagonal nanosheets formed at 80 °C contained less than 20% of the hexagonal nanosheets (Figure 6). Furthermore, no Au sample could be obtained when the temperature was 60 °C. The reaction profile in the MW system with different temperatures was monitored (Supporting Information Figure S3). When the temperature was 100 °C, the pressure of the system could reach to 250 psi, while the maximum of pressure was 200 and 30 psi at 80 and 60 °C, respectively.

Other surfactants, such as PVP and SDS, were also used for the synthesis of Au samples. The similar structures of Au samples were obtained despite the use of PVP, 0.16, 0.08, 0.04, and 0.02 g, as Figure 7 shows. However, more uniform and better dispersed Au nanoparticles were formed by using more PVP, according to the size distribution of Au nanoparticles in


dx.doi.org/10.1021/sc400007p | ACS Sustainable Chem. Eng. 2013, 1, 810–816

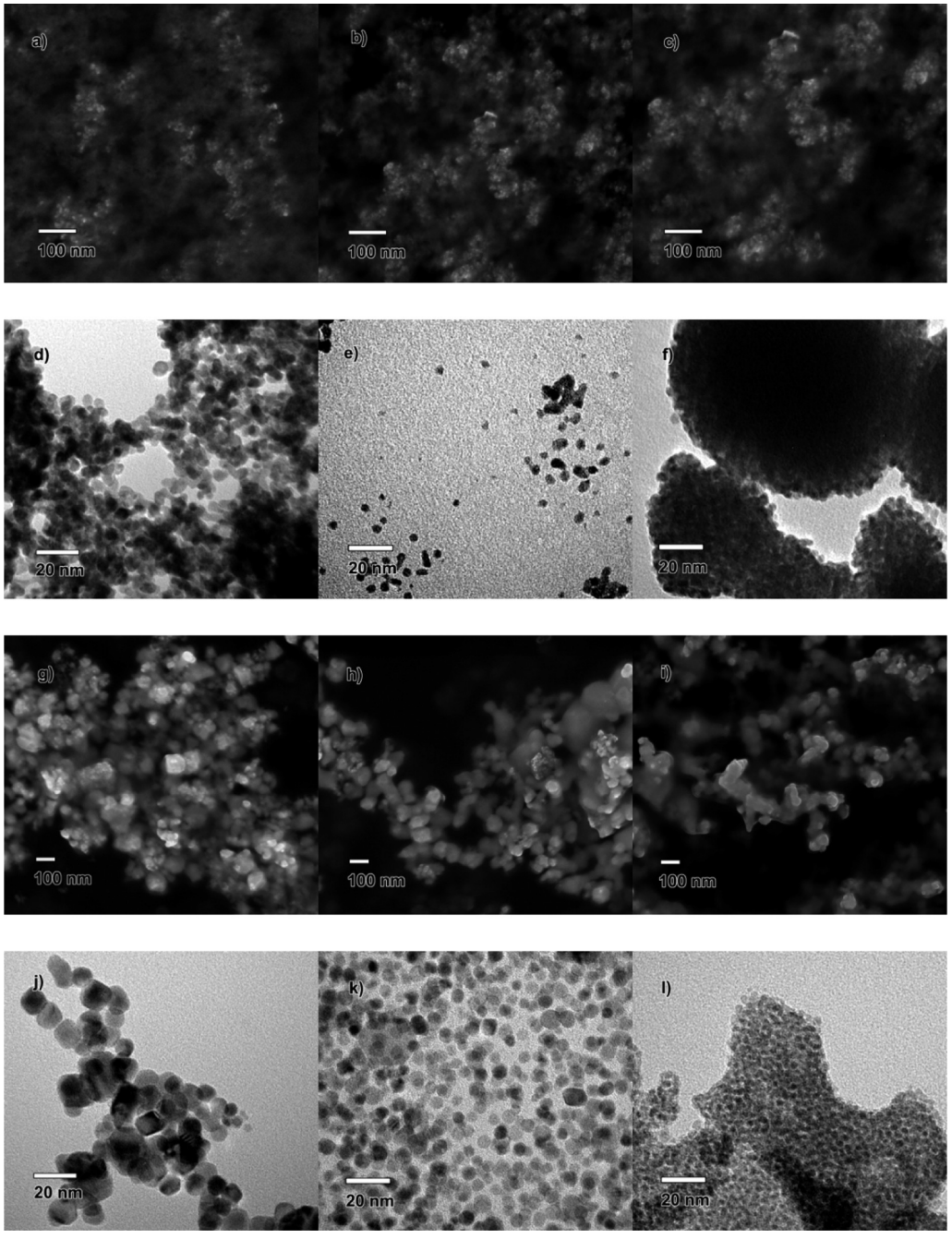


**Figure 11.** (a) SEM image of Pt at 2 min. (b) SEM image of Pt at 30 min. (c) SEM image of Pt at 2 min with SDS. (d) TEM image of Pt at 2 min. (e) TEM image of Pt at 2 min with PVP. (f) TEM image of Pt at 2 min with CTAB. (g) SEM image of Pd at 2 min. (h) SEM image of Pd at 30 min. (i) SEM image of Pd at 2 min with SDS. (j) TEM image of Pd at 2 min. (k) TEM image of Pd at 2 min with PVP. (l) TEM image of Pd at 2 min with CTAB.

the presence of 0.16 (Figure 7e) and 0.02 g (Figure 7f) PVP. The maximum size of that of 0.16 g PVP is about 450 nm, while that of 0.02 g PVP is about 600 nm. Most Au nanoparticles are about 190−330 nm both in the presence of 0.16 and 0.02 g PVP, which account for 75% and 50% of the total, respectively, which prove the better uniformity of obtained Au nanoparticles using 0.16 than 0.02 g PVP.

In the presence of SDS, Au nanosheets were formed but could not get uniform structure by changing its content (Figure 8). When SDS was 0.075 mmol, just nanoparticles were obtained. With the increasing of SDS amount, Au nanosheets appeared in the products. Also, their percentage composition could be enhanced by using more SDS. The shapes of Au nanosheets are not hexagonal but triangular, which are different from that in the presence of CTAB.

The MW-assisted glycerol method is general and can be extended to other noble metals such as Pt and Pd. The Pt peaks at $2\theta$ = 39.7, 46.3, and 67.3 correspond to (111), (200), and (220) (PDF no. 01-1190); the peaks at 40.4, 46.8, and 68.4 can be assigned to (111), (200), and (220) planes of the Pd crystal (PDF no. 01-1201) (Figure 9). However, under conventional heating conditions, no powder appeared in the case of Pt, which is similar to that of Au, while nano Pd was formed partially (Figure 10). This indicates that $PdCl_2$ is easier to be

reduced than $HAuCl_4$ and $HPtCl_6$ with glycerol. Figure 11 displays the SEM and TEM images of Pt and Pd samples. Without any surfactant, the sizes of Pt obtained at 2 and 30 min are similar (~5 nm), while the sizes of Pd are bigger than that of Pt (~10 nm). The sizes of Pd and Pt did not change with prolonged time. The morphology of both Pd and Pt were not affected by SDS; both sizes and shapes had no obvious difference with and without using SDS. However, the addition of CTAB and PVP influence the morphology of Pd and Pt a little bit. In the presence of PVP, the formed Pd and Pt have excellent dispersity, and the sizes of Pt and Pd are 3−10 and 5−15 nm, respectively. With CTAB, the obtained Pt and Pd tend to aggregate more to generate clusters, and the sizes of Pd are similar to Pt nanoparticles (about 3−5 nm), which is different from the facts obtained using SDS or PVP.

The catalytic conversion of 4-nitrophenol to 4-aminophenol was used as a model to investigate the potential catalytic properties of as-prepared Au nanosheets (Figure 12). 4-Aminophenol was

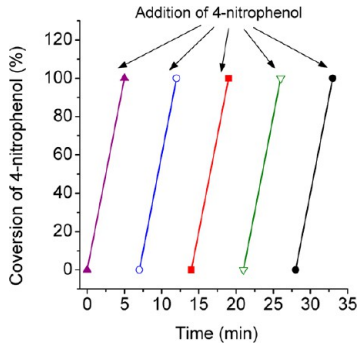


**Figure 12.** Catalytic activity and recyclability of as-prepared Au nanosheets.

not formed in the absence of the catalyst even after 30 min, while 4-nitrophenol was quantitatively converted to 4-aminophenol within 5 min after addition of Au nanosheets. Moreover, the catalytic durability of Au nanosheets was found to be excellent; 4-nitrophenol could be completely reduced within 5 min for each cycle even after five runs, thus implying the good stable catalytic performance of Au nanosheets.

## CONCLUSION

In summary, a newer application of glycerol, whose generation is dramatically increasing with the rapid development of biodiesel industry, was explored in the field of synthesis of nanomaterials. Glycerol can act as a reducing agent for the fabrication of noble metals, such as Au, Pt, and Pd, under MW irradiation. The shapes of ensuing particles can be changed by adding various surfactants. In the presence of CTAB, Au nanosheets were formed within 2 min, and the size of nanosheet can be controlled by the MW irradiation time and glycerol content.

## ASSOCIATED CONTENT

### Supporting Information

Reaction profiles in the microwave system. This material is available free of charge via the Internet at http://pubs.acs.org.

## AUTHOR INFORMATION

### Corresponding Author

*E-mail address: Varma.Rajender@epa.gov (R.S.V.); koujiahui@gmail.com (J.K.). Tel.: +1-513-487-2701.

### Notes

The authors declare no competing financial interest.

## ACKNOWLEDGMENTS

J.K. is a postdoctoral research participant at the National Risk Management Research Laboratory, Environmental Protection Agency, administered by the Oak Ridge Institute for Science and Education (ORISE).

## REFERENCES

(1) Chatzifragkou, A.; Papanikolaou, S. Effect of impurities in biodiesel-derived waste glycerol on the performance and feasibility of biotechnological processes. *Appl. Microbio. Biotechnol.* **2012**, *95*, 13−27.

(2) Dam, J.; Hanefeld, U. Renewable Chemicals: Dehydroxylation of Glycerol and Polyols. *Chemsuschem* **2011**, *4*, 1017−1034.

(3) Yang, F.; Hanna, M. A.; Sun, R. Value-added uses for crude glycerol-a byproduct of biodiesel production. *Biotechnol. Biofuels* **2012**, *5*, 13.

(4) Abad, S.; Turon, X. Valorization of biodiesel derived glycerol as a carbon source to obtain added-value metabolites: Focus on polyunsaturated fatty acids. *Biotechnol. Adv.* **2012**, *30*, 733−741.

(5) Guo, S.; Wang, E. Noble metal nanomaterials: Controllable synthesis and application in fuel cells and analytical sensors. *Nano Today* **2011**, *6*, 240−264.

(6) Garnett, E. C.; Cai, W.; Cha, J. J.; Mahmood, F.; Connor, S. T.; Christoforo, M. G.; Cui, Y.; McGehee, M. D.; Brongersma, M. L. Self-limited plasmonic welding of silver nanowire junctions. *Nat. Mater.* **2012**, *11*, 241−249.

(7) Zhu, Z.; Meng, H.; Liu, W.; Liu, X.; Gong, J.; Qiu, X.; Jiang, L.; Wang, D.; Tang, Z. Superstructures and SERS Properties of Gold Nanocrystals with Different Shapes. *Angew. Chem.-Inter. Ed.* **2011**, *50*, 1593−1596.

(8) Chiu, C.-Y.; Li, Y.; Ruan, L.; Ye, X.; Murray, C. B.; Huang, Y. Platinum nanocrystals selectively shaped using facet-specific peptide sequences. *Nature Chem.* **2011**, *3*, 393−399.

(9) White, R. J.; Luque, R.; Budarin, V. L.; Clark, J. H.; Macquarrie, D. J. Supported metal nanoparticles on porous materials. Methods and applications. *Chem. Soc. Rev.* **2009**, *38*, 481.

(10) Campelo, J. M.; Luna, D.; Luque, R.; Marinas, J. M.; Romero, A. A. Sustainable preparation of supported metal nanoparticles and their applications in catalysis. *Chemsuschem* **2009**, *2*, 18.

(11) Dahl, J. A.; Maddux, B. L. S.; Hutchison, J. E. Toward greener nanosynthesis. *Chem. Rev.* **2007**, *107*, 2228.

(12) Yang, H.; Shen, C.; Song, N.; Wang, Y.; Yang, T.; Gao, H.; Cheng, Z. Facile synthesis of hollow nano-spheres and hemispheres of cobalt by polyol reduction. *Nanotechnology* **2010**, *21*, 375602.

(13) Herricks, T.; Chen, J. Y.; Xia, Y. N. Polyol synthesis of platinum nanoparticles: Control of morphology with sodium nitrate. *Nano Lett.* **2004**, *4*, 2367−2371.

(14) Sun, Y. G.; Mayers, B.; Herricks, T.; Xia, Y. N. Polyol synthesis of uniform silver nanowires: A plausible growth mechanism and the supporting evidence. *Nano Lett.* **2003**, *3*, 955−960.

(15) Cable, R. E.; Schaak, R. E. Low-temperature solution synthesis of nanocrystalline binary intermetallic compounds using the polyol process. *Chem. Mater.* **2005**, *17*, 6835−6841.

(16) Jiu, J.; Suganuma, K.; Nogi, M. Effect of additives on the morphology of single-crystal Au nanosheet synthesized using the polyol process. *J. Mater. Sci.* **2011**, *46* (14), 4964−4970.

(17) Coskun, S.; Aksoy, B.; Unalan, H. E. Polyol Synthesis of Silver Nanowires: An Extensive Parametric Study. *Cryst.Growth Des.* **2011**, *11*, 4963−4969.

(18) Nizami, A. N.; Rahman, M. A.; Ahmed, N. U.; Islam, M. S. Whole Leea macrophylla ethanolic extract normalizes kidney deposits and recovers renal impairments in an ethylene glycol-induced urolithiasis model of rats. *Asian Pac. J. Trop. Med.* **2012**, *5*, 533−538.

(19) Porter, W. H. Ethylene glycol poisoning: Quintessential clinical toxicology; analytical conundrum. *Clin. Chim. Acta* **2012**, *413* (3−4), 365−377.
(20) Kou, J.; Varma, R. S. Speedy fabrication of diameter-controlled Ag nanowires using glycerol under microwave irradiation conditions. *Chem. Commun.* **2013**, *49*, 692−694.
(21) Smith, D. K.; Miller, N. R.; Korgel, B. A. Iodide in CTAB Prevents Gold Nanorod Formation. *Langmuir* **2009**, *25*, 9518−9524.
(22) Tyler, T. P.; Lin, P. A.; Tian, Y.; Gao, H.-J.; Gao, X. P. A.; Sankaran, R. M.; Hersam, M. C. Centrifugal Shape Sorting of Faceted Gold Nanoparticles Using an Atomic Plane-Selective Surfactant. *J. Phys. Chem. Lett.* **2012**, *3*, 1484−1487.
(23) Zhong, L.; Zhou, X.; Bao, S.; Shi, Y.; Wang, Y.; Hong, S.; Huang, Y.; Wang, X.; Xie, Z.; Zhang, Q. Rational design and SERS properties of side-by-side, end-to-end and end-to-side assemblies of Au nanorods. *J. Mater. Chem.* **2011**, *21*, 14448−14455.
(24) Bullen, C.; Zijlstra, P.; Bakker, E.; Gu, M.; Raston, C. Chemical Kinetics of Gold Nanorod Growth in Aqueous CTAB Solutions. *Cryst.Growth Des.* **2011**, *11*, 3375−3380.
(25) Kah, J. C. Y.; Zubieta, A.; Saavedra, R. A.; Hamad-Schifferli, K. Stability of Gold Nanorods Passivated with Amphiphilic Ligands. *Langmuir* **2012**, *28*, 8834−8844.
(26) Dallinger, D.; Kappe, C. O. Microwave-assisted synthesis in water as solvent. *Chem. Rev.* **2007**, *107*, 2563−2591.
(27) Mehtaa, V. P.; Van der Eycken, E. V. Microwave-assisted C-C bond forming cross-coupling reactions: an overview. *Chem. Soc. Rev.* **2011**, *40*, 4925−4936.
(28) Baghbanzadeh, M.; Carbone, L.; Cozzoli, P. D.; Kappe, C. O. Microwave-Assisted Synthesis of Colloidal Inorganic Nanocrystals. *Angew. Chem.-Inter. Ed.* **2011**, *50*, 11312−11359.
(29) Rosana, M. R.; Tao, Y.; Stiegman, A. E.; Dudley, G. B. On the rational design of microwave-actuated organic reactions. *Chem. Sci.* **2012**, *3*, 1240−1244.
(30) Patzke, G. R.; Zhou, Y.; Kontic, R.; Conrad, F. Oxide Nanomaterials: Synthetic Developments, Mechanistic Studies, and Technological Innovations. *Angew. Chem.-Inter. Ed.* **2011**, *50*, 826−859.
(31) Modeshia, D. R.; Walton, R. I. Solvothermal synthesis of perovskites and pyrochlores: crystallisation of functional oxides under mild conditions. *Chem. Soc. Rev.* **2010**, *39*, 4303−4325.
(32) Cundy, C. S.; Cox, P. A. The hydrothermal synthesis of zeolites: History and development from the earliest days to the present time. *Chem. Rev.* **2003**, *103*, 663−701.
(33) Kou, J.; Saha, A.; Bennett-Stamper, C.; Varma, R. S. Inside-out core-shell architecture: controllable fabrication of $Cu_2O$@Cu with high activity for the Sonogashira coupling reaction. *Chem.Commun.* **2012**, *48*, 5862−5864.